Unquenched Lattice Landau Gauge QCD Simulation

Sadataka Furui *
School of Science and Engineering, Teikyo University
Hideo Nakajima[†]
Department of Information science, Utsunomiya University

16 Dec. 2004, Workshop at RCCP Tsukuba

*e-mail furui@umb.teikyo-u.ac.jp
[†]e-mail nakajima@is.utsunomiya-u.ac.jp

- Why unquenched Landau gauge QCD?
- The Gribov copy problem
- The reflection positivity (sample wise) and the Kugo-Ojima parameter
  - Quenched SU(3) $\beta = 6.0, 6.4, 6.45,\ 16^4, 24^4, 32^4, 48^4, 56^4$
  - Unquenched SU(3) $\beta = 5.2,\ 20^3 \times 48$ Wilson action(JLQCD)
  - Unquenched SU(3) $\beta = 2.1,\ 24^3 \times 48$ Iwasaki action(CP-PACS)
  - Unquenched SU(3) $\beta = 6.76, 6.83,\ 20^3 \times 64$ KS-fermion(MILC)
  - Unquenched SU(3) $\beta = 5.415,\ 16^3 \times 32$ KS-fermion(ILDG)

- The ghost propagator

- The gluon propagator

- Kugo-Ojima parameter

- QCD running coupling

- $\tilde{Z}_1$ of the lattice QCD

- Discussion and conclusion

I. Introduction

- Why unquenched Landau gauge QCD?
  - Is the Kugo-Ojima confinement scenario independent of the presence of matter fields?
  - Are there problems specific to the quenched lattice simulation?
  - Are there infrared fixed point of the running coupling? What is the role of fermions in the running coupling of QCD?
  - Do all simulation with different kinds of fermions yield the same physical quantities in the continuum limit? (Wilson, Kogut-Susskind, Ginsparg-Wilson, Neuberger)

– Is the extra taste degrees of freedom of staggered fermion properly treated in the lattice?

– Is a unified picture of dynamical chiral symmetry breaking and confinement through the running coupling possible?

– Is the lattice result consistent with continuum theory (DSE,ERGE)?

Issues of Landau gauge QCD.

- The running coupling and the Kugo-Ojima parameter
  S.Furui and H.Nakajima(Confinement IV in Vienna 2000)

- Continuum limit of lattice vs DSE and/or ERGE results
  von Smekal, Hauck and Alkofer(1998), Paulowski et al.(2003), Kato(2004)

  - Infrared exponent κ v.s. lattice exponent α_G
    Fischer, Alkofer and Reinhardt(2002)

  - Infrared fixed point α_0 of the running coupling
    Lerche and von Smekal(2002), Bloch(2002,2003), Kondo(2003)

  - Vertex renormalization factor $\tilde{Z}_1$ of the lattice QCD
    Bloch, Cucchieri, Langfeld, Mendes(2002)

- PMS or effective charge method for evading Landau pole.
  Stevenson(1981), Grunberg(1984)

- Application to lattice.
  Chetyrkin and Rétay(2000), van Acoleyen(2002), F.N.(2004)

- The fundamental modular region and the Gribov boundary
  Cucchieri(1997), Zwanziger(2003)

- Reflection positivity and the global rotational symmetry
  - Gribov copy dependence
  - Quenched and Unquenched difference
- The finite size effect
  - Symmetric hypercubic lattice and asymmetric lattice
  - Wilson action, Iwasaki action vs Staggered Lüscher-Weisz action

- Two types of the gauge field definitions:

  1. $\log U$ type: $U_{x,\mu} = e^{A_{x,\mu}}$, $A^{\dagger}_{x,\mu} = -A_{x,\mu}$,

  2. U linear type: $A_{x,\mu} = \frac{1}{2}(U_{x,\mu} - U^{\dagger}_{x,\mu})|_{trlp.}$,

  ($A_\mu(x) = i \sum_a A_\mu{}^a(x) \frac{\Lambda^a}{\sqrt{2}}$, $tr \Lambda^a \Lambda^b = \delta^{ab}$.)

- The optimizing function

  1. $F_U(g) = ||A^g||^2 = \sum_{x,\mu} \mathrm{tr} \left(A^g{}_{x,\mu}{}^{\dagger} A^g_{x,\mu} \right)$,

  2. $F_U(g) = \sum_{x,\mu} \left(1 - \frac{1}{3} \mathrm{Re}\ \mathrm{tr} U^g_{x,\mu} \right)$,

- Stationality(Landau gauge), Local minimum(Gribov Region), Global minimum(Fundamental modular(FM) region)

- The covariant derivativative $D_\mu(U)$ for two options
  $D_\mu(U_{x,\mu})\phi = S(U_{x,\mu})\partial_\mu\phi + [A_{x,\mu}, \bar{\phi}]$
  where $\partial_\mu\phi = \phi(x+\mu) - \phi(x)$, and $\bar{\phi} = \dfrac{\phi(x+\mu)+\phi(x)}{2}$,

- The definition of operation $S(U_{x,\mu})B_{x,\mu}$

  1. $S(U_{x,\mu})B_{x,\mu} = T(\mathcal{A}_{x,\mu})B_{x,\mu}$

     where $\mathcal{A}_{x,\mu} = adj_{A_{x,\mu}} = [A_{x,\mu}, \cdot]$, $T(x) = \dfrac{x/2}{\mathrm{th}(x/2)}$.

  2. $S(U_{x,\mu})B_{x,\mu} = \dfrac{1}{2}\left\{\dfrac{U_{x,\mu}+U^\dagger_{x,\mu}}{2}, B_{x,\mu}\right\}\Big|_{trlp.}$

- The Kugo-Ojima confinement criterion

$$
\begin{aligned}
&(\delta_{\mu\nu} - \frac{q_\mu q_\nu}{q^2}) u^{ab}(q^2) \\
&= \frac{1}{V} \sum_{x,y} e^{-ip(x-y)} \langle \mathrm{tr} \left(\Lambda^{a\dagger} D_\mu \frac{1}{-\partial D} [A_\nu, \Lambda^b] \right)_{xy} \rangle. \qquad (1)
\end{aligned}
$$

- The fact that the parameter c defined as $u^{ab}(0) = -\delta^{ab} c$ becomes 1 is the confinement criterion. The parameter c is related to the renormalization factor as

$$
1 - c = \frac{Z_1}{Z_3} = \frac{\tilde{Z}_1}{\tilde{Z}_3} \qquad (2)
$$

- If the finiteness of $\tilde{Z}_1$ is proved, divergence of $\tilde{Z}_3$ is a sufficient condition. If Z_3 vanishes in the infrared, Z_1 should have higher order 0.

- Zwanziger's horizon condition

$$\sum_{x,y} e^{-ip(x-y)} \left\langle \mathrm{tr}\left(\Lambda^{a\dagger} D_\mu \frac{1}{-\partial D}(-D_\nu)\Lambda^b\right)_{xy}\right\rangle$$

$$= G_{\mu\nu}(p)\delta^{ab} = \left(\frac{e}{d}\right)\frac{p_\mu p_\nu}{p^2}\delta^{ab} - \left(\delta_{\mu\nu} - \frac{p_\mu p_\nu}{p^2}\right)u^{ab},$$

where $e = \left\langle \sum_{x,\mu} \mathrm{tr}(\Lambda^{a\dagger} S(U_{x,\mu})\Lambda^a)\right\rangle / \{(n^2-1)V\}$, and the horizon condition reads $\lim_{p\to 0} G_{\mu\mu}(p) - e = 0$, and the l.h.s. of the condition is $\left(\frac{e}{d}\right)+(d-1)c-e = (d-1)h$ where $h = c-\frac{e}{d}$ and dimension $d = 4$, and it follows that $h = 0 \rightarrow$ horizon condition, and thus the horizon condition coincides with Kugo-Ojima criterion provided the covariant derivative approaches the naive continuum limit, i.e., $e/d = 1$.

- Unquenched SU(3) configurations
  - Wilson action: $W_{1\times1}$ (JLQCD)

$$q_\mu{}^W = \frac{2}{a}\sin(\frac{\widehat{q}_\mu a}{2})$$

  - Iwasaki action: $c_0 W_{1\times1} + c_1 W_{2\times1}$ (CP-PACS)

$$q_\mu{}^I = \frac{2}{a}\sqrt{\sin^2(\frac{\widehat{q}_\mu a}{2}) + \frac{1}{3}\sin^4(\frac{\widehat{q}_\mu a}{2})} \qquad (3)$$

  - Staggered Lüscher-Weisz action: $c_0 W_{1\times1} + c_1 W_{2\times1} + c_2 W_{1\times1\times1}$ (MILC)

- Comparison of JLQCD, CP-PACS and MILC

Table 1: β, κ and the sea quark mass m^{VWI}(vector Ward identity) and the inverse lattice constant $1/a$.

	β	$\kappa_{u,d}$	am^{VWI}/am_s^{VWI}	N_f	$1/a(GeV)$
JLQCD(h)	5.2	0.1340	0.134	2	2.221
JLQCD(l)	5.2	0.1355	0.093	2	2.221
CP-PACS(h)	2.1	0.1340	0.087	2	1.834
CP-PACS(l)	2.1	0.1357	0.020	2	1.834
MILC(h)	6.83(β_{imp})		0.040/0.050	2+1	1.644
MILC(l)	6.76(β_{imp})		0.007/0.050	2+1	1.644
ILDG	5.415		0.025	2	1.140

II. The Gribov copy problem

- In the Langevin formulation of QCD, Zwanziger conjectures that the path integral over the FM region will become equivalent to that over the Gribov region in the continuum. This conjecture is consistent with the view that the boundary of the FMG and that of the Gribov region overlaps and the probability distribution is accumulated in this overlapped region.
- On the lattice, when β and the lattice size is not large enough, Gribov noise of copies i.e. statistical weight of the copies is crucial for extracting sample averages.

- The FMG fixing via parallel tempering method works nicely. SU(2) $\beta = 2.2$, 16^4. (67 samples).
- The FMG configurations and the 1st copy which is in the Gribov region but not necessarily in the FM region have the following differences:
  1) The absolute value of the Kugo-Ojima parameter c of the FMG is smaller than that of the 1st copy.
  2) The singularity of the ghost propagator of the FMG is less than that of the 1st copy.
  3) The gluon propagator of the two copies are almost the same within statistical errors.
  4) The horizon function deviation parameter h of the FMG is not closer to 0, i.e. the value expected in the continuum limit, than that of the 1st copy.

III. The reflection positivity and the Kugo-Ojima parameter

- The gluon propagator on the lattice

$$
\begin{aligned}
D_{A,\mu\nu}(q) &= \frac{2}{n^2-1} tr\langle \tilde{A}_\mu(q)\tilde{A}_\nu(q)^\dagger\rangle \\
&= (\delta_{\mu\nu} - \frac{q_\mu q_\nu}{q^2}) D_A(q^2), \qquad (4)
\end{aligned}
$$

where $\tilde{A}_\mu(q) = \frac{1}{\sqrt{V}}\sum_x e^{-iqx}A_\mu(x)$.

- We choose q transverse to μ, and since there are 3 possible choices of $\nu \neq \mu$, we define $D_A(q^2)_\mu$:

$$
D_A(q^2) = \frac{1}{3}\sum_\mu \sum_{\nu\neq\mu} \frac{1}{3}\frac{2}{n^2-1} tr\langle \tilde{A}_\mu(q_\nu)\tilde{A}_\mu(q_\nu)^\dagger\rangle = \frac{1}{3}\sum_\mu D_A(q^2)_\mu \qquad (5)
$$

- We make an average of the three combinations and make the discrete Fourier transform of the correlater $D_A(q^2)_\mu$, which can be compared with the Schwinger function:

$$S(t,\vec{0}) = \frac{1}{\sqrt{L}} \sum_{q_0=0}^{L-1} D_A(q_0,\vec{0}) e^{2\pi i q_0 t/L} \tag{6}$$

- Gribov copy dependence of the 1-d Fourier transform of the sample-wise gluon propagator of exceptional samples.

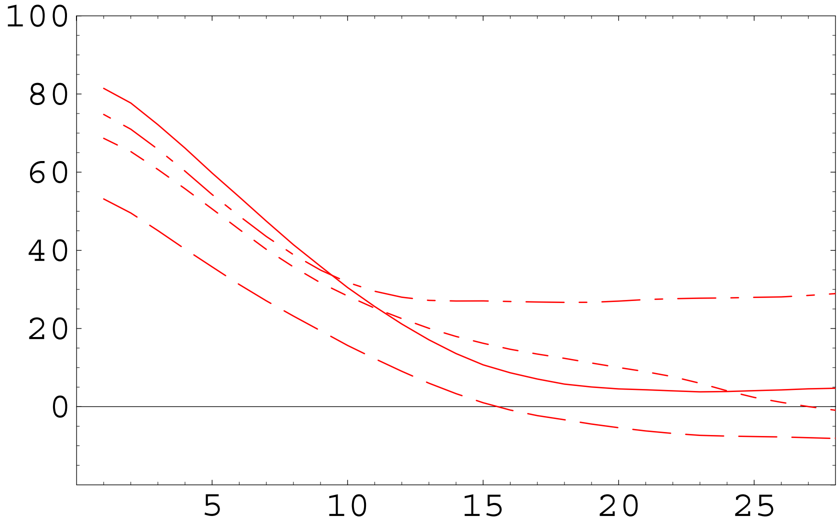

Fig. 1: The 1-d FT of the gluon propagator $D_A(q^2)_\mu$. $\beta = 6.4$, 56^4 in the $\log U$ definition. sample I_A

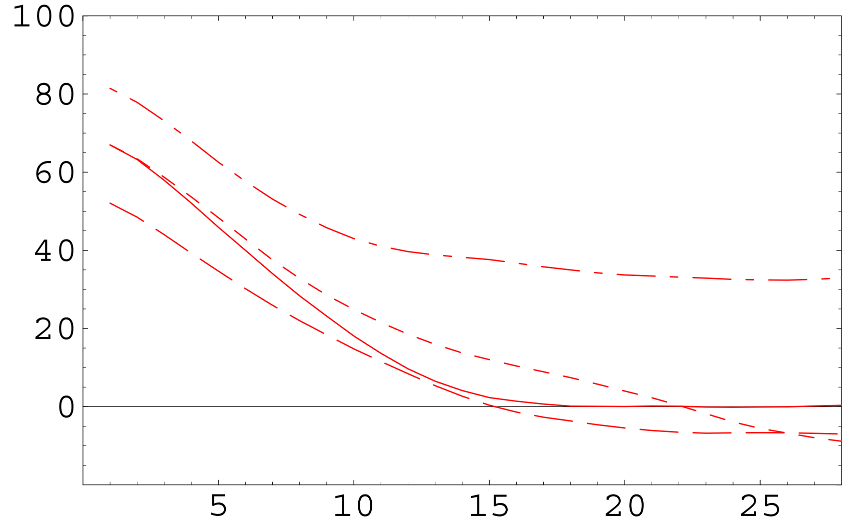

Fig. 2: The 1-d FT of the gluon propagator $D_A(q^2)_\mu$. $\beta = 6.4$, 56^4 in the $\log U$ definition. sample I_B

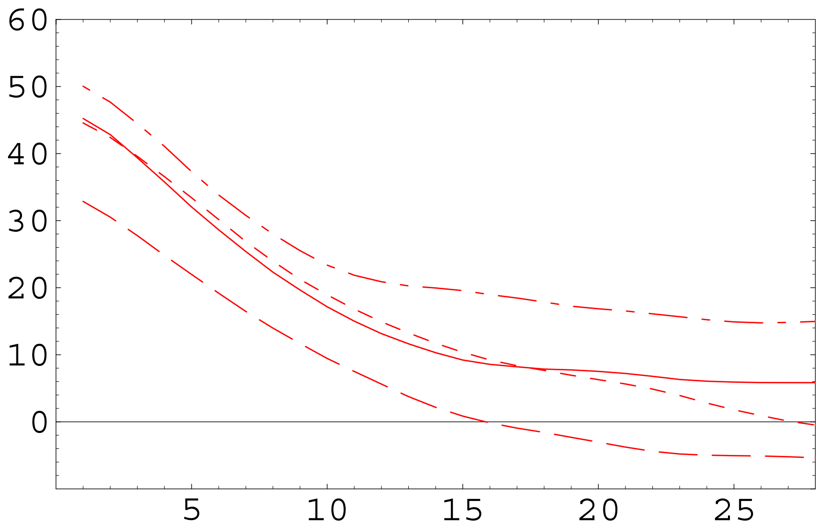

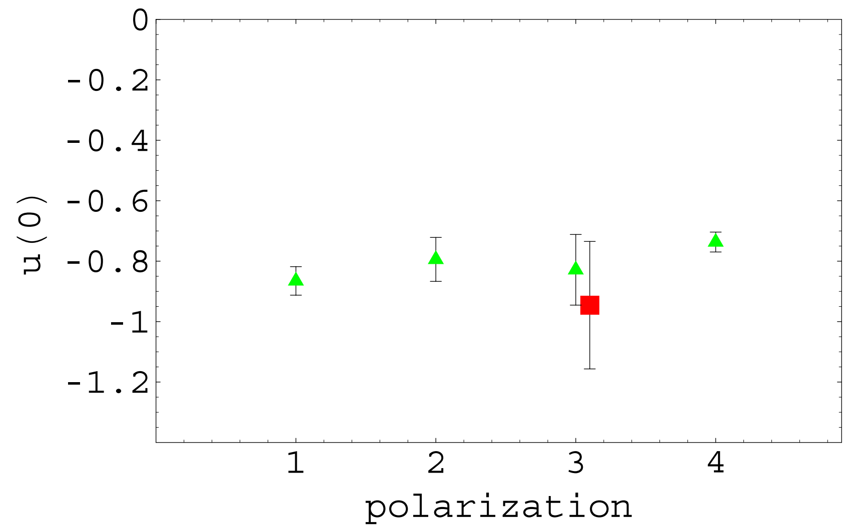

Fig. 3a:The 1-d FT of the gluon propagator $D_A(q^2)_\mu$. Solid line:$\mu = 1$, Dotted line:$\mu = 2$, Dashed line:$\mu = 3$, Dash-dotted line:$\mu = 4$. $\beta = 6.4$, 56^4. Sample $\overline{I_A}$.

Fig. 3b:The polarization dependence of the Kugo-Ojima parameter $\beta = 6.4$, 56^4. The average of the Cartan subalgebra components is plotted by the box. Sample $\overline{I_A}$.

- An average of the 4 components does not violate reflection positivity.

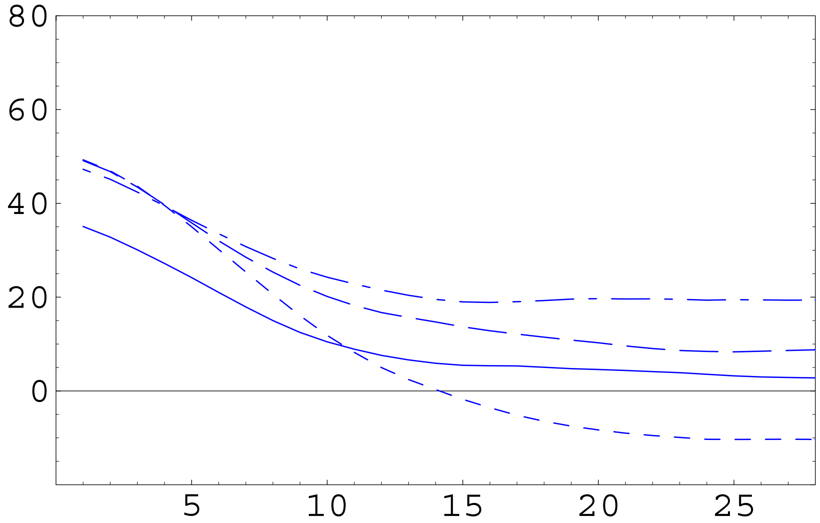

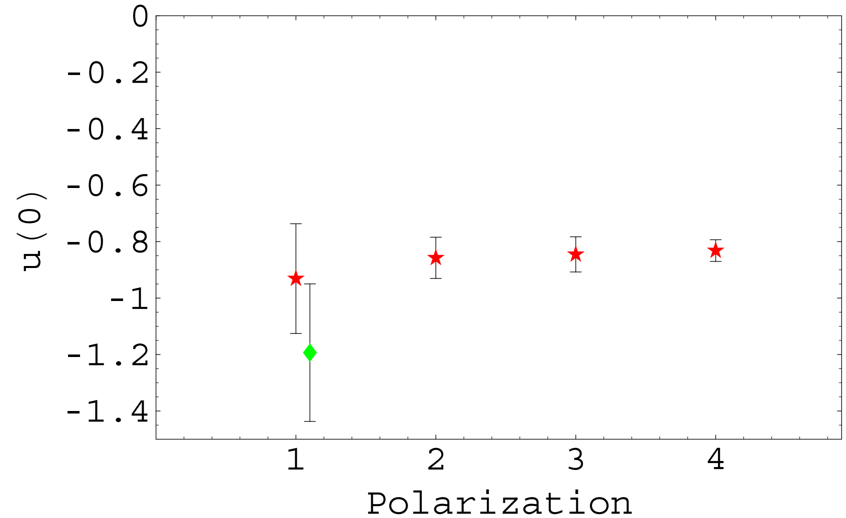

Fig. 4a:The 1-d FT of the gluon propagator $D_A(q^2)_\mu$. Solid line:$\mu = 1$, Dotted line:$\mu = 2$, Dashed line:$\mu = 3$, Dash-dotted line:$\mu = 4$. $\beta = 6.45$, 56^4. Sample III.

Fig. 4b:The polarization dependence of the Kugo-Ojima parameter $\beta = 6.45$, 56^4. The average of the Cartan subalgebra components is plotted by the diamond. Sample III.

- An average of the 4 components does not violate reflection positivity.

Table 1:The Gribov copy dependence of the Kugo-Ojima parameter c, trace divided by the dimension e/d, horizon condition deviation parameter h and the exponent α_G.

	I_A	I_B	II_A	II_B	average
$\Vert A\Vert^2$	0.09081	0.09079	0.090698	0.090695	0.09072(7)
c	0.851(77)	0.837(58)	0.835(53)	0.829(56)	0.827(15)
e/d	0.9535(1)	0.9535(1)	0.9535(1)	0.9535(1)	0.954(1)
h	-0.102(77)	-0.117(58)	-0.118(53)	-0.125(56)	-0.127(15)
α_G	0.272	0.241	0.223	0.221	0.223

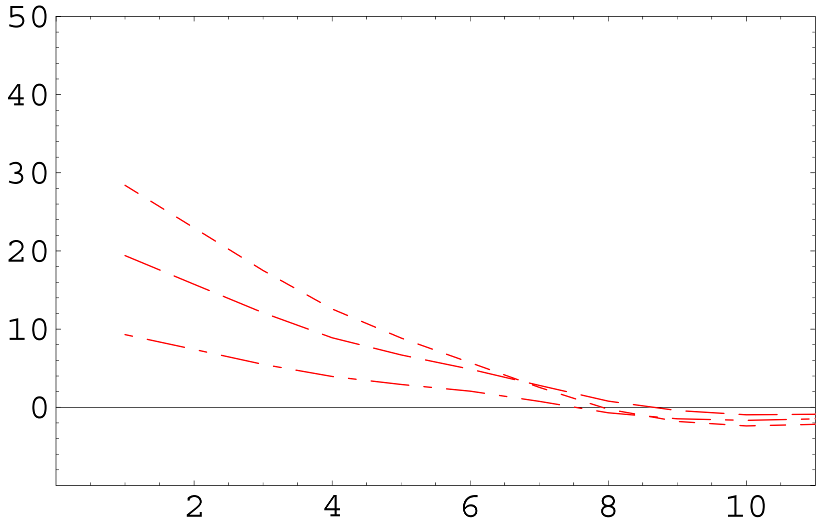

Fig. 5a: The 1-d FT of the gluon propagator $D_A(q^2)_m$. (Dash-dotted line:m=1, Dashed line:m=2, Dotted line:m=3). $K_{sea} = 0.1340$.

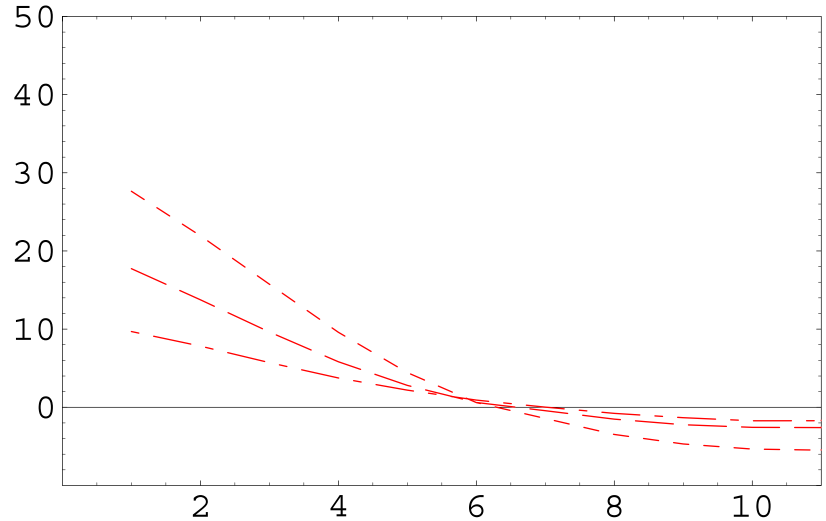

Fig. 5b: The 1-d FT of the gluon propagator $D_A(q^2)_m$ (Dash-dotted line:m=1, Dashed line:m=2, Dotted line:m=3). $K_{sea} = 0.1355$.

- The average of the components violate reflection positivity.
- The position of zero approaches closer to the origin for lighter quarks.

IV. The ghost propagator

- Ghost propagator

$$\begin{aligned} FT[D_G^{ab}(x,y)] &= FT\langle tr(\Lambda^a\{(\mathcal{M}[U])^{-1}\}_{xy}\Lambda^b\rangle, \\ &= \delta^{ab}D_G(q^2) \end{aligned} \tag{7}$$

- The ghost dressing function $G(q^2)$

$$D_G(q^2) = \frac{G(q^2)}{q^2}. \tag{8}$$

- $M\widetilde{O}M$ scheme

$$D_G(q^2) = -\frac{Z_g(q^2,y)|_{y=0.02142}}{q^2} = \frac{G(q^2)}{q^2}. \tag{9}$$

- The PMS and the effective charge method

  In the PMS method, the n th order approximation to the physical quantity $\mathcal{R}$ is expressed by the corresponding series of coupling constant $h^{(n)}$ which is defined as a solution of

$$
\begin{aligned}
\beta_0 \log \frac{\mu^2}{\Lambda^2} &= \frac{1}{h} + \frac{\beta_1}{\beta_0} \log(\beta_0 h) \\
&\quad + \int_0^h dx \left(\frac{1}{x^2} - \frac{\beta_1}{\beta_0 x} - \frac{\beta_0}{\beta_0 x^2 + \beta_1 x^3 + \cdots + \beta_n x^{n+2}} \right) \qquad (10)
\end{aligned}
$$

  where the scheme independent constant and the logarithmic term are separated.

  When $\mathcal{R}$ is the QCD running coupling from the triple gluon vertex from up to three loop diagrams in the $\overline{MS}$ scheme,

$$\mathcal{R}^n = h^{(n)}(1 + A_1 h^{(n)} + A_2 h^{(n)2} + \cdots + A_n h^{(n)n}) \qquad (11)$$

where in the case of $n = 3$, $A_1 = 70/3$, $A_2 = \frac{516217}{576} - \zeta_3 \frac{153}{4}$, $A_3 = \frac{304676635}{6912} - \zeta_3 \frac{299961}{64} - \zeta_5 \frac{81825}{64}$.

When one defines $y_{\overline{MS}}(q)$ as a solution of

$$1/y_{\overline{MS}}(q) = \beta_0 \log(q/\Lambda_{\overline{MS}})^2 - \frac{\beta_1}{\beta_0} \log(\beta_0 y_{\overline{MS}}(q)) \qquad (12)$$

and express the solution of (10)

$$\begin{aligned} h(q) &= y_{\overline{MS}}(q)(1 + y_{\overline{MS}}(q)^2(\bar{\beta}_2/\beta_0 - (\beta_1/\beta_0)^2) \\ &+ y_{\overline{MS}}(q)^3 \frac{1}{2}(\bar{\beta}_3/\beta_0 - (\beta_1/\beta_0)^3) + \cdots \end{aligned} \qquad (13)$$

where $\beta_0 = 11, \beta_1 = 102$, $\bar{\beta}_2 = \frac{2857}{2}$, $\bar{\beta}_3 = \frac{149753}{6} + 3564\zeta_3$, we can calculate $\mathcal{R}$ via eq.(11)

The parameter $y_{\overline{MS}}(q)$ can be expressed as y defined as a solution of (Λ characterizes the scale of the system)

$$\beta_0 \log \frac{\mu^2}{\Lambda^2} = \frac{1}{y(\mu)} + \frac{\beta_1}{\beta_0} \log(\beta_0 y(\mu)) \tag{14}$$

and the function

$$k(q^2, y) = \frac{1}{y} + \frac{\beta_1}{\beta_0} \log(\beta_0 y) - \beta_0 \log(q^2/\Lambda^2_{\overline{MS}}). \tag{15}$$

- Ghost propagator, Quenched

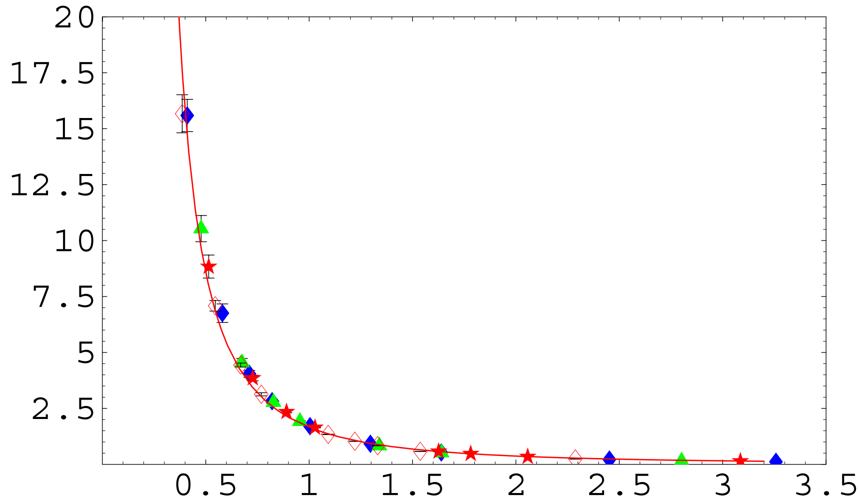

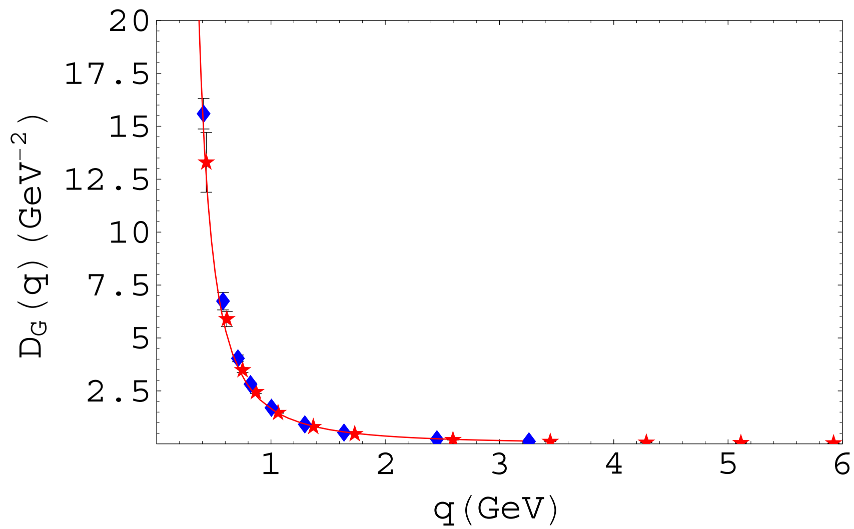

Fig. 6: The ghost propagator as the function of the momentum q(GeV). $\beta = 6.0$, 24^4(stars),32^4(unfilled diamonds),$\beta = 6.4$, 48^4(triangles) and 56^4(filled diamond) in the $\log U$ definition. The fitted line is that of the $\widetilde{\mathrm{MOM}}$ scheme.

Fig. 7:The ghost propagator as the function of the momentum q(GeV). $\beta = 6.45$, 56^4(stars) and $\beta = 6.4, 56^4$(filled diamonds) in the $\log U$ definition.

- Ghost dressing function, Quenched

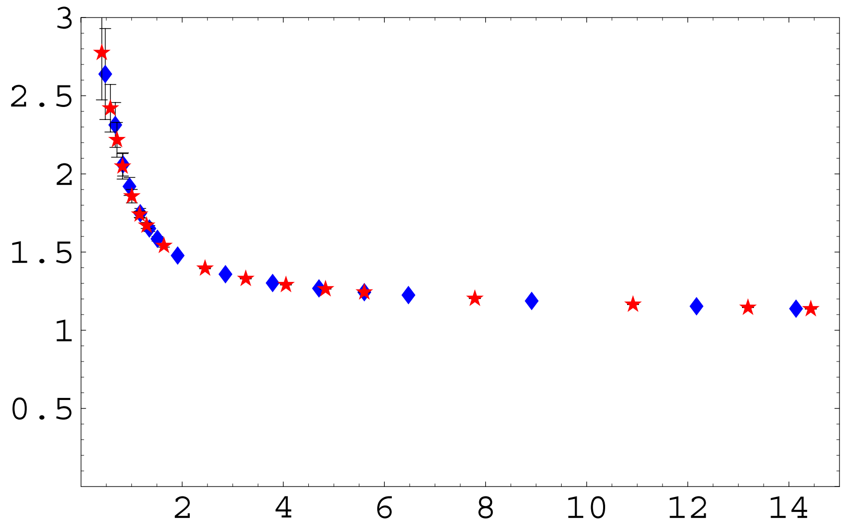

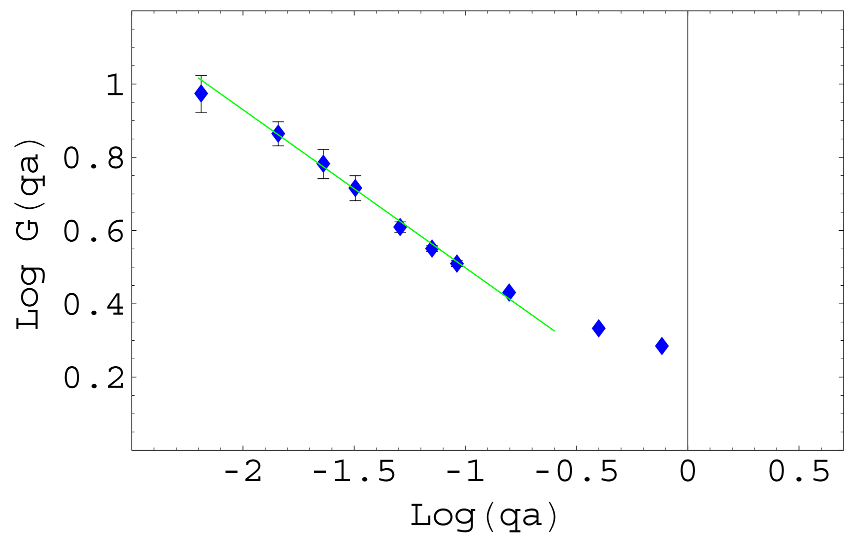

Fig 8a: The ghost dressing function as the function of the momentum q(GeV). $\beta = 6.4$, 48^4(triangles) and 56^4(filled diamonds) in the $U-$linear definition.

Fig 8b: The log of ghost dressing function as the function of $\log(qa)$(GeV). $\beta = 6.4$, 56^4 in the $U-$linear definition. $\alpha_G = 0.22$.

- Ghost propagator, Unquenched(JLQCD)

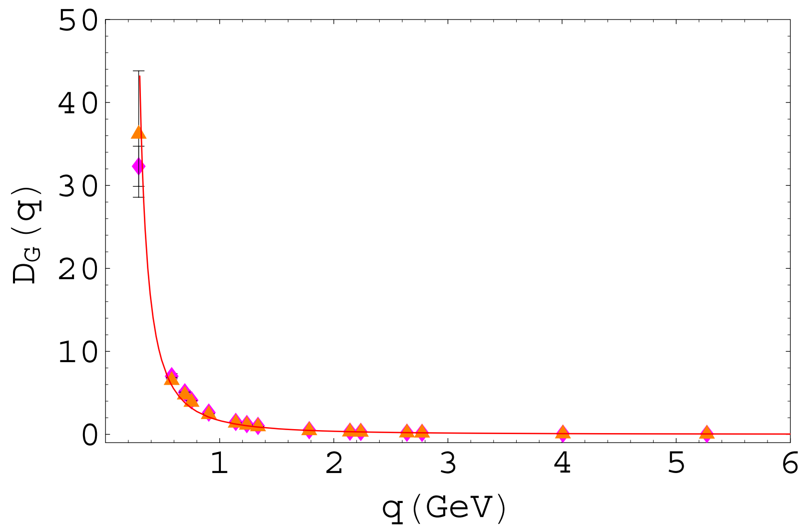

Fig.9: $D_G(q)$ as a function of q(GeV). Wilson action $K_{sea} = 0.1340$ (diamonds) and 0.1355 (triangles).

• Ghost propagator, Unquenched (CP-PACS, MILC)

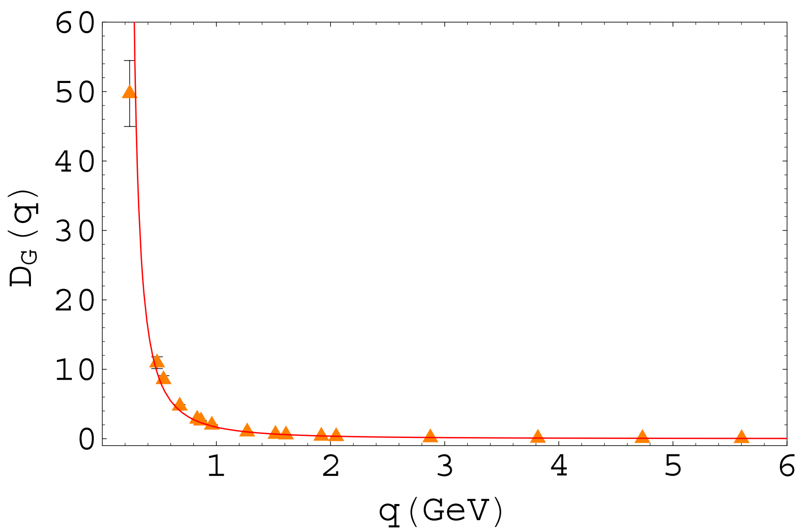

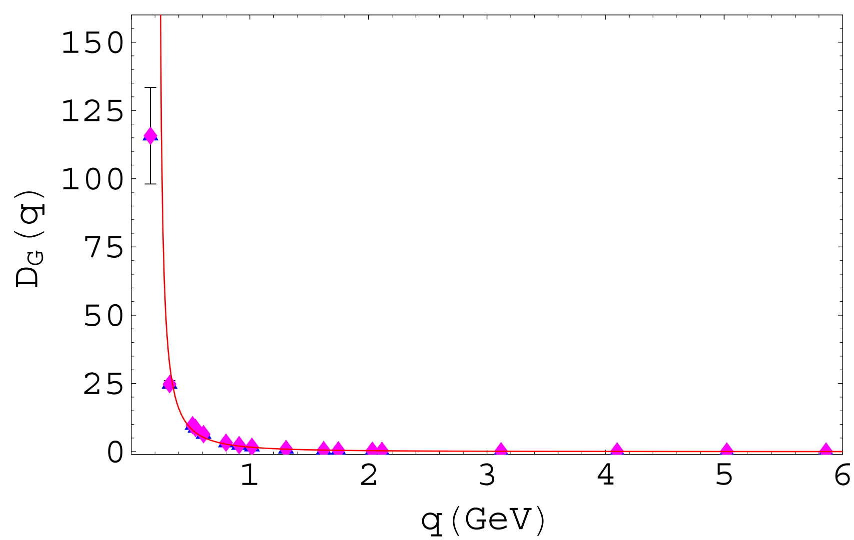

Fig.10a: $D_G(q)$ of the CP-PACS of $K_{sea} = 0.1357$ (diamonds) and 0.1382 (triangles). (10 samples) The $\widetilde{MOM}$ scheme(red line).

Fig.10b: $D_G(q)$ of the MILC $\beta_{imp} = 6.83, am_{u,d} = 0.040$(diamonds) and 6.76,$am_{u,d} = 0.007$(triangles). (50 samples)

- Ghost dressing function, Unquenched (CP-PACS, MILC)

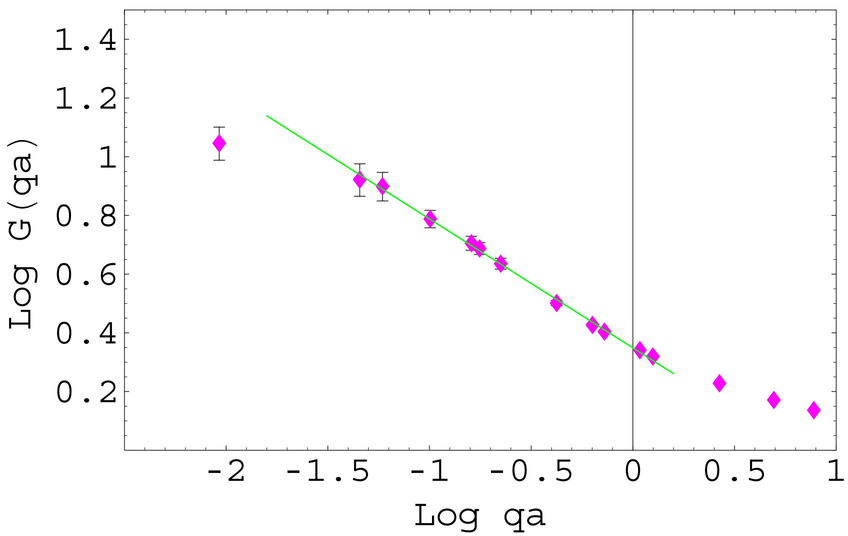

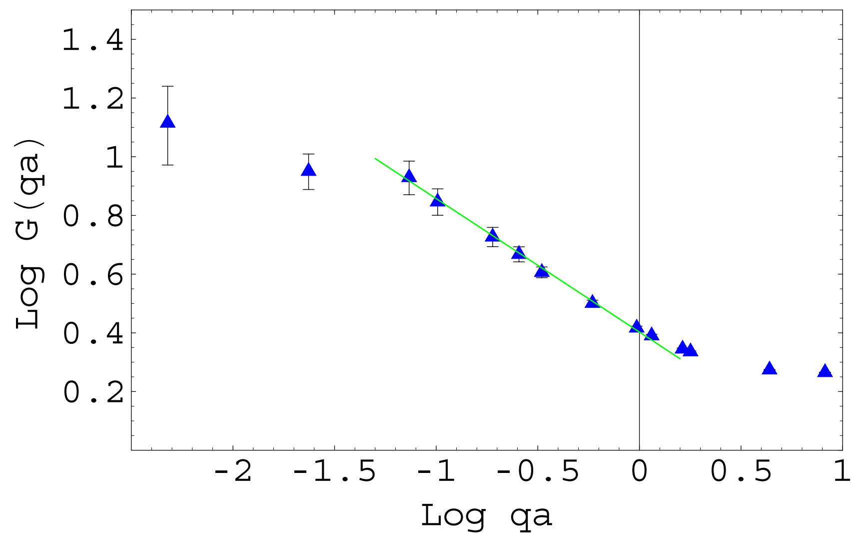

Fig.11a: $\log G(qa)$ as the function of $\log(qa)$ of the CP-PACS $K_{sea} = 0.1357$ (diamonds). (10 samples). $\alpha_G = 0.22$

Fig.11b: $\log G(qa)$ as the function of $\log(qa)$ of the MILC $\beta_{imp} = 6.76$,a $m_{u,d} = 0.007$(triangles). (50 samples). $\alpha_G = 0.23$

- Ghost propagator, Unquenched(JLQCD,CP-PACS and MILC)

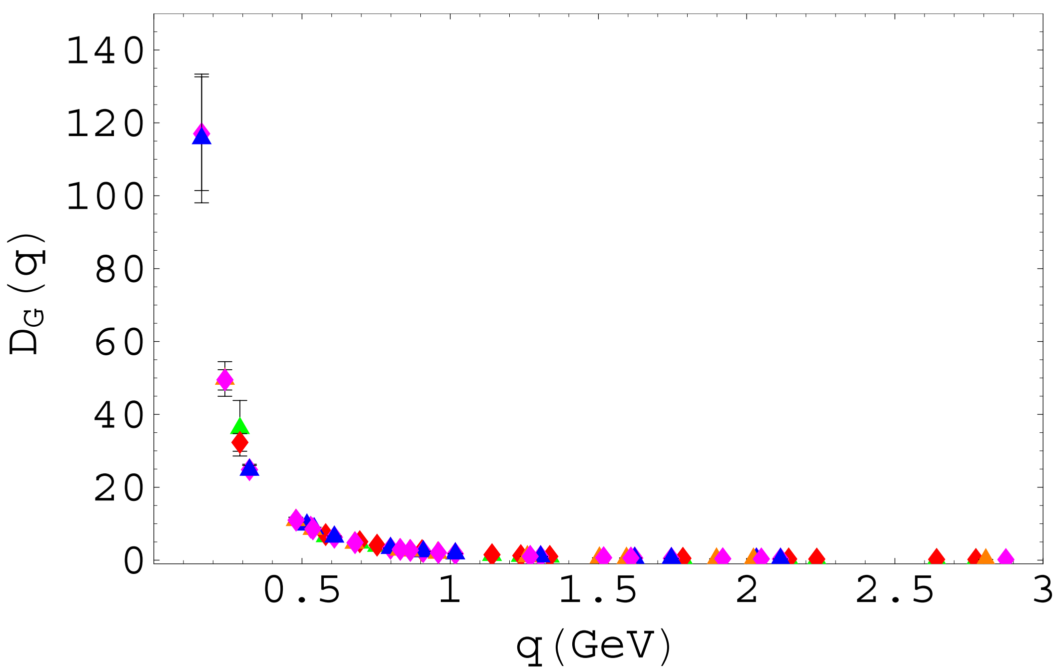

Fig.12: $D_G(q)$ as a function of q(GeV). Unquenched JLQCD, CP-PACS and MILC.

V. The gluon propagator

- Gluon propagator

$$
\begin{aligned}
D^{ab}_{A,\mu\nu}(q) &= 2 \sum_{x=\mathbf{x},t} e^{-iqx} \langle A_\mu{}^a(x) A_\nu{}^b(0) \rangle \\
&= (\delta_{\mu\nu} - \frac{q_\mu q_\nu}{q^2}) D_A(q^2) \delta^{ab},
\end{aligned} \tag{16}
$$

- The gluon dressing function $Z(q^2)$

$$
D_A(q^2) = \frac{Z(q^2)}{q^2}, \tag{17}
$$

- We choose q following the cylinder cut.

- Gluon, Quenched($\beta = 6.45$)

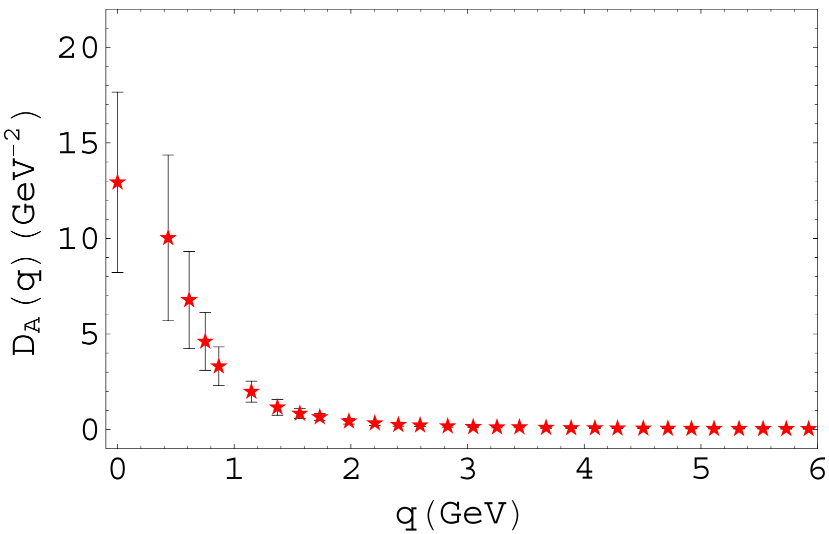

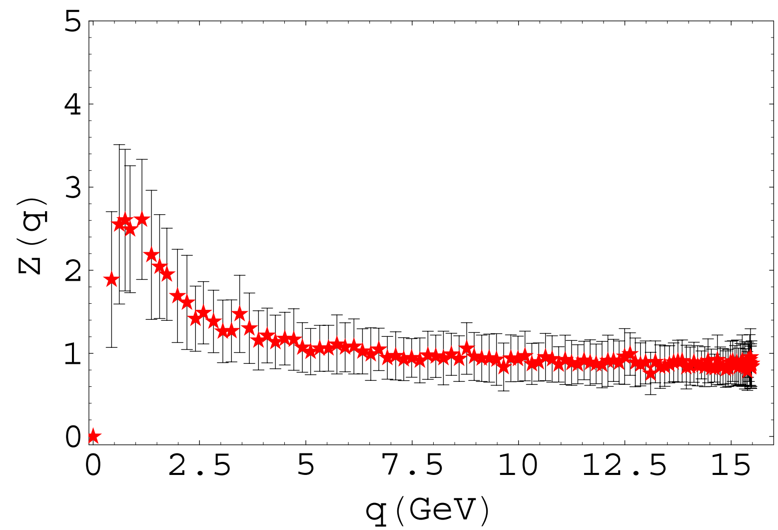

Fig.13a: $D_A(q)$ as a function of q(GeV).

Fig.13b: $Z(q)$ as a function of q(GeV).

• Gluon, Unquenched(JLQCD)

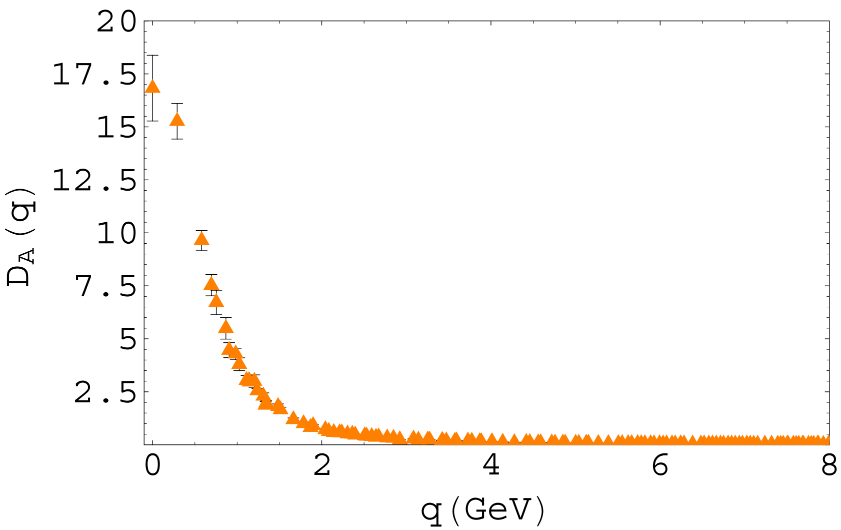

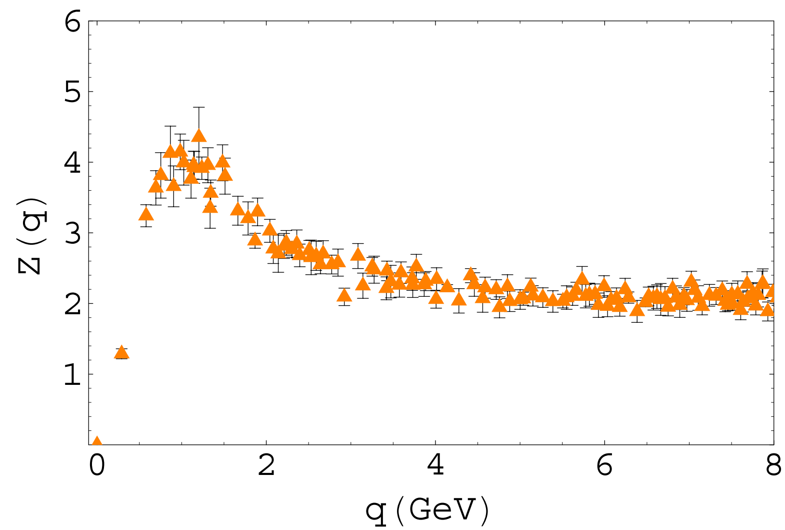

Fig.14a: $D_A(q)$ as a function of q(GeV).

Fig.14b: $Z(q)$ as a function of q(GeV).

• Gluon, Unquenched(CP-PACS)

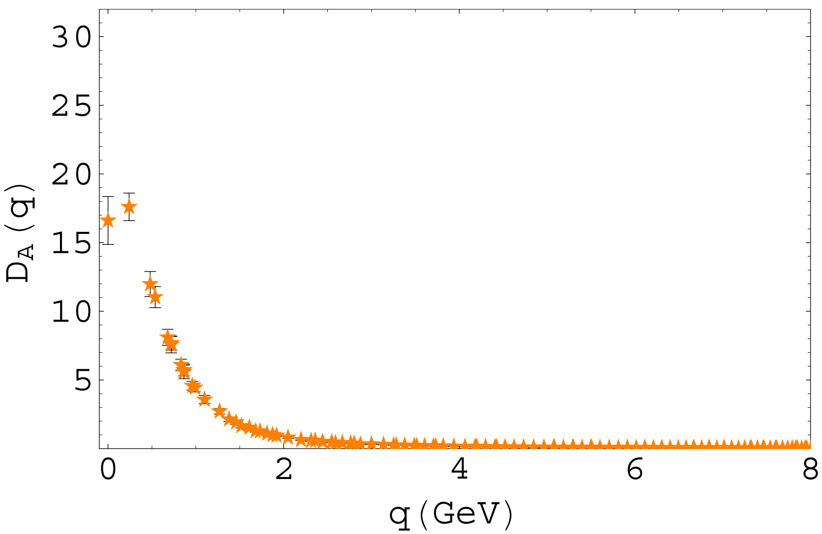

Fig.15a: $D_A(q)$ as a function of q(GeV).

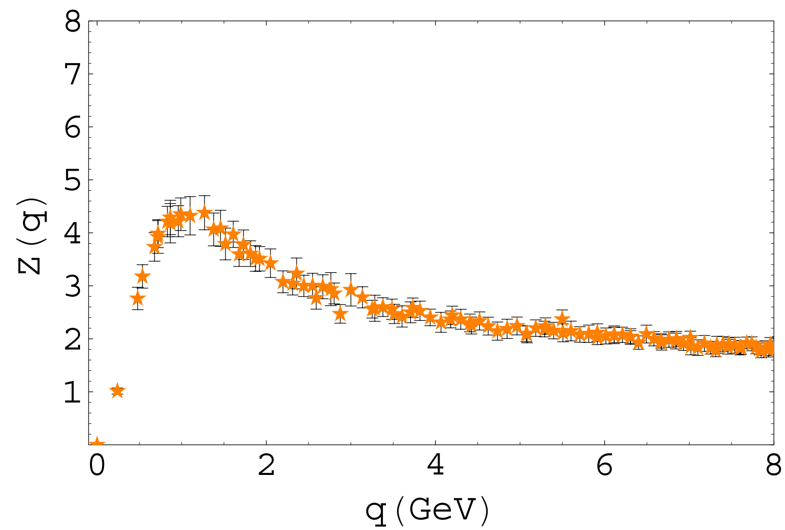

Fig.15b: $Z(q)$ as a function of q(GeV).

• Gluon, Unquenched(MILC)

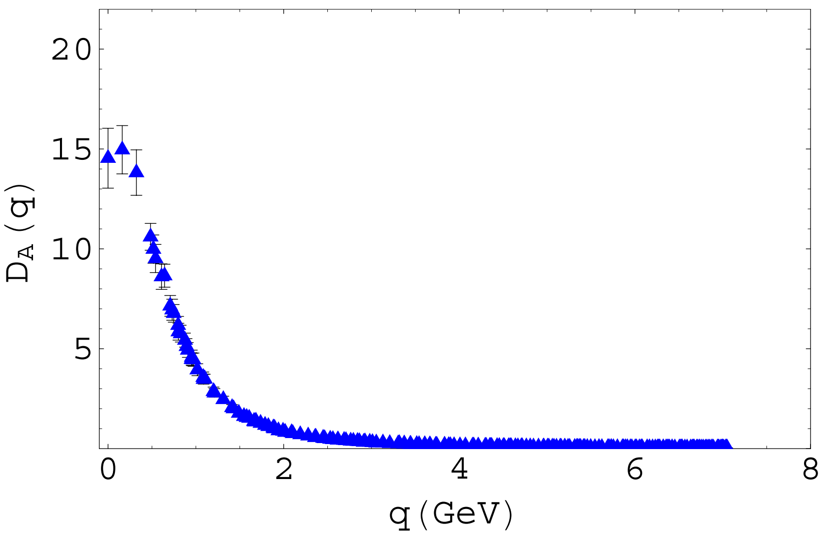

Fig.16a: $D_A(q)$ as a function of q(GeV).

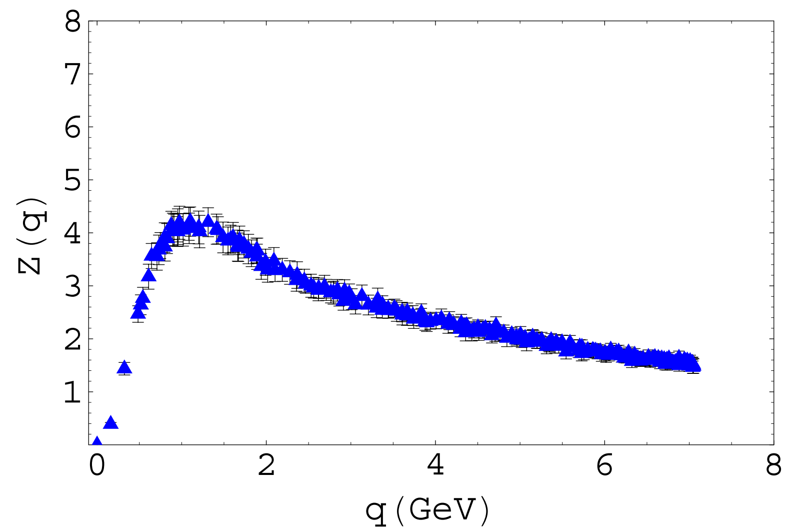

Fig.16b: $Z(q)$ as a function of q(GeV).

VI. Kugo-Ojima parameter

- Kugo-Ojima parameter

$$
\begin{aligned}
&(\delta_{\mu\nu} - \frac{q_\mu q_\nu}{q^2}) u^{ab}(q^2) \\
&= \frac{1}{V} \sum_{x,y} e^{-ip(x-y)} \langle \mathrm{tr} \left(\Lambda^{a\dagger} D_\mu \frac{1}{-\partial D} [A_\nu, \Lambda^b] \right)_{xy} \rangle.
\end{aligned}
\tag{18}
$$

Table 2: The Kugo-Ojima parameter c in $\log U$(β =6.0,6.4 and 6.45) and $U-$linear definition($\beta = 6.0$ and 6.4.)

β	L	c_1	e_1/d	h_1	c_2	e_2/d	h_2
6.0	16	0.628(94)	0.943(1)	-0.32(9)	0.576(79)	0.860(1)	-0.28(8)
6.0	24	0.774(76)	0.944(1)	-0.17(8)	0.695(63)	0.861(1)	-0.17(6)
6.0	32	0.777(46)	0.944(1)	-0.16(5)	0.706(39)	0.862(1)	-0.15(4)
6.4	32	0.700(42)	0.953(1)	-0.25(4)	0.650(39)	0.883(1)	-0.23(4)
6.4	48	0.793(61)	0.954(1)	-0.16(6)	0.739(65)	0.884(1)	-0.15(7)
6.4	56	0.827(27)	0.954(1)	-0.12(3)	0.758(52)	0.884(1)	-0.13(5)
6.45	56	0.809(81)	0.954(1)	-0.15(8)			

• Kugo-Ojima parameter, Unquenched

Table 3: The Kugo-Ojima parameter along the spacial directions c_x and that along the time axis c_t and the average c, trace divided by the dimension e/d, horizon function deviation h of quenched Wilson action , unquenched Wilson action , unquenched Wilson improved action , unquenched KS improved action and unquenched KS Wilson.

K_{sea} or β	c_x	c_t	c	e/d	h
β =6.4	0.827(27)	0.827(27)	0.827(27)	0.954(1)	-0.12(3)
β =6.45	0.809(81)	0.809(81)	0.809(81)	0.954(1)	-0.15(8)
K_{sea} =0.1340	0.887(87)	0.723(38)	0.846(106)	0.930(1)	-0.084(106)
K_{sea} =0.1355	1.005(217)	0.670(47)	0.921(238)	0.934(1)	-0.013(238)
K_{sea} =0.1357	0.859(58)	0.763(36)	0.835(68)	0.9388(1)	-0.104(68)
K_{sea} =0.1382	0.887(87)	0.723(38)	0.846(106)	0.9409(1)	-0.095(106)
β_{imp} =6.76	1.040(111)	0.741(28)	0.965(162)	0.9325(1)	-0.032(162)
β_{imp} =6.83	1.012(153)	0.754(28)	0.947(174)	0.9339(1)	-0.013(174)
β =5.415	0.835(72)	0.735(35)	0.810(78)	0.924(1)	-0.114(78)

VII. QCD running coupling

- The methods to calculate the running coupling
  - NRQCD (strength of the heavy quark potential)
  - Schrödinger functional(response to the variation)
  - Triple gluon vertex in Landau gauge /in 'instanton scheme'
  - Gluon-ghost-antighost vertex in Landau gauge
- Our running coupling $\alpha_s(q)$

$$\alpha_s(q^2) = \frac{g_0^2}{4\pi}\frac{Z(q^2)G(q^2)^2}{\tilde{Z}_1^2} \sim \alpha_s(\Lambda_{UV})(qa)^{-2(\alpha_D+2\alpha_G)}. \qquad (19)$$

- The scale was fitted from the perturbative QCD in the highest lattice momentum region.

• $\alpha_s(q)$, Quenched

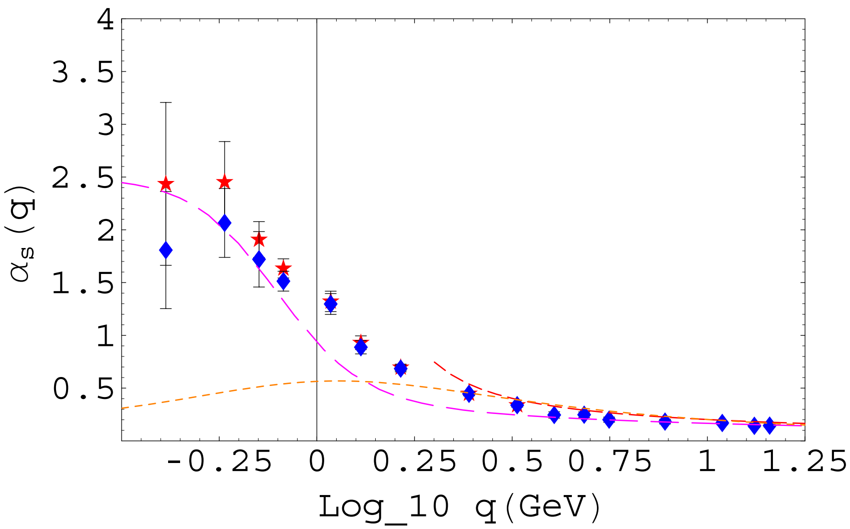

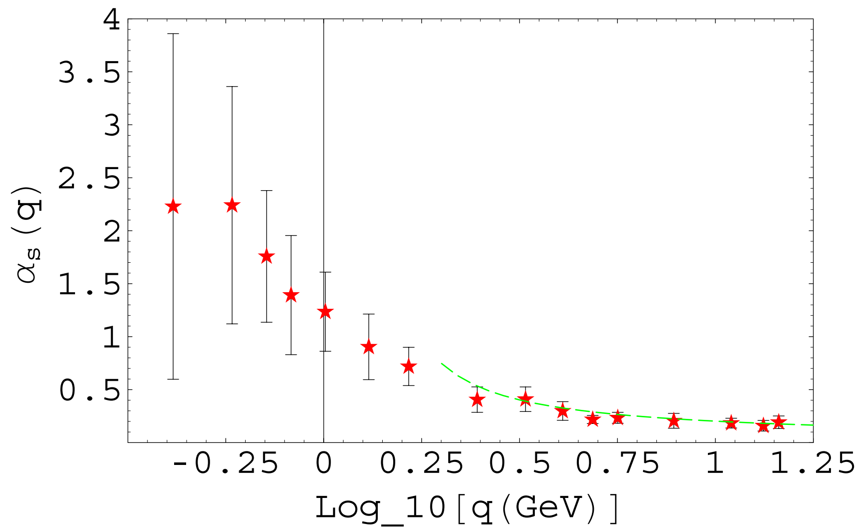

Fig 17a: $\alpha_s(q)$ as a function of $\log_{10} q$(GeV) of $\beta = 6.4$, 56^4 with the ghost propagator of the I_A copy (stars) and the average (diamonds). DSE(long dashed line), pQCD(short dashed line), contour improved perturbation method (dotted line).

Fig.17b: $\alpha_s(q)$ as a function of $\log_{10} q$(GeV). Quenched $\beta = 6.45$, 56^4 lattice. (10 samples). The pQCD (with c/q^2 term. dash dotted line)

- $\alpha_s(q)$, Unquenched (JLQCD)

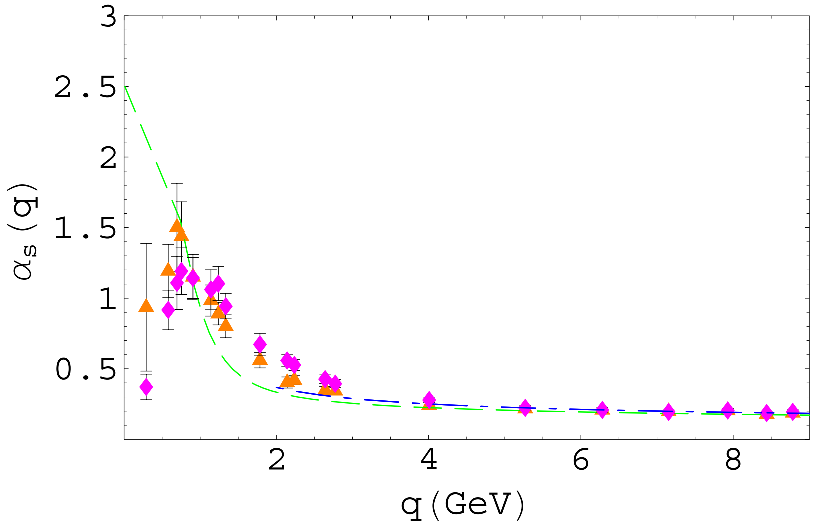

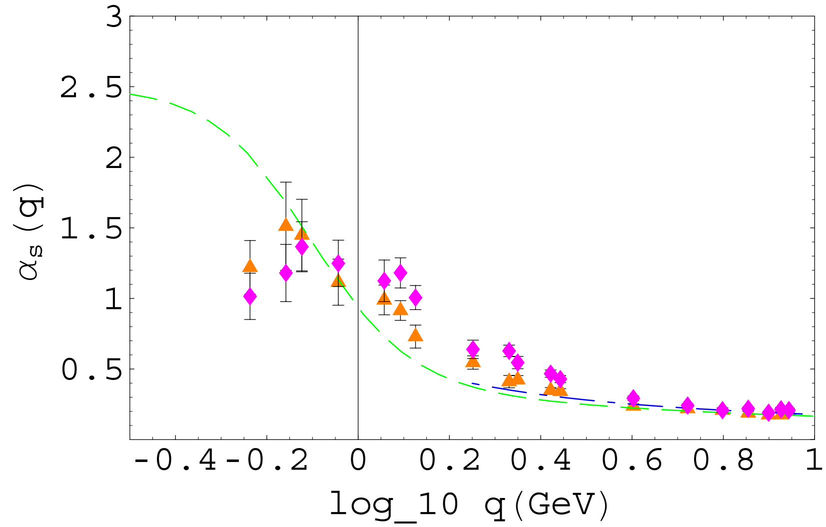

Fig.18a: $\alpha_s(q)$ of the JLQCD of K_{sea} = 0.1340 (diamonds) and 0.1355 (triangles). (25 samples) The DSE with $\alpha_0 = 2.5$(long dashed line), pQCD (no c/q^2 term. dash dotted line).

Fig.18b: Same as Fig.18a as the function of $\log_{10}[q(GeV)]$

- $\alpha_s(q)$, Unquenched (CP-PACS)

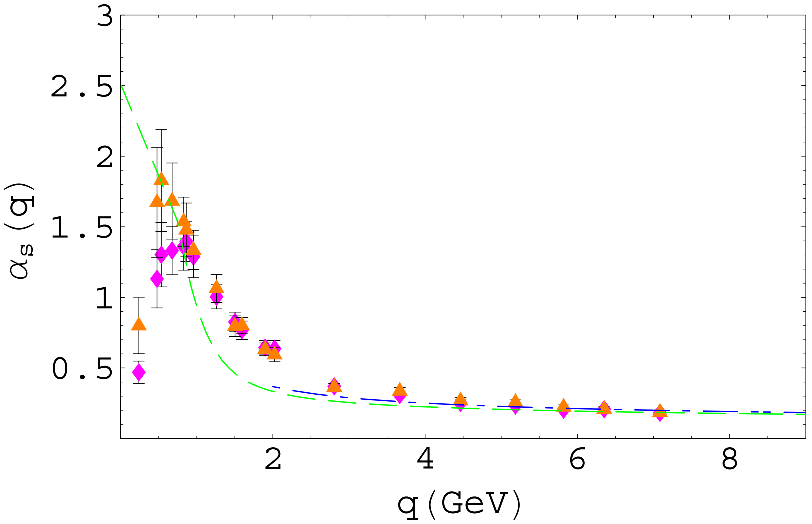

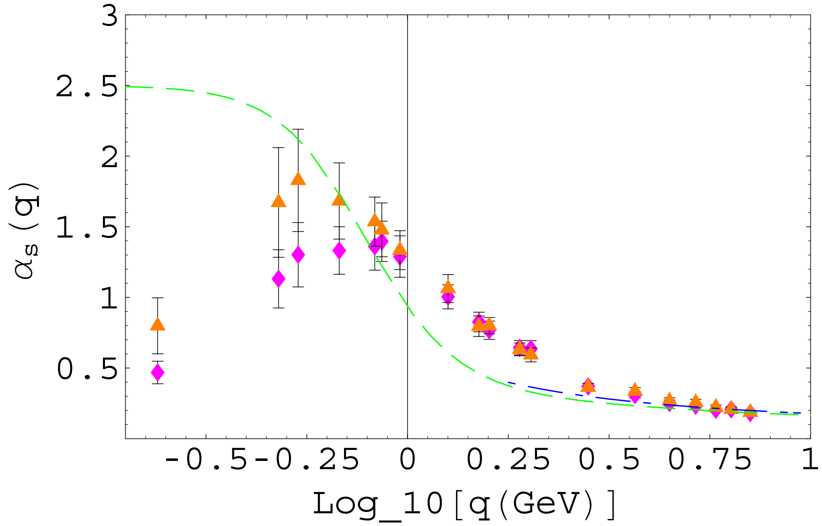

Fig.19a: $\alpha_s(q)$ of the CP-PACS of $K_{sea} = 0.1357$ (diamonds) and 0.1382 (triangles). (25 samples) The DSE approach with $\alpha_0 = 2.5$(long dashed line), pQCD (dash dotted line).

Fig.19b: Same as Fig.19a as the function of $\log_{10}[q(GeV)]$

• $\alpha_s(q)$, Unquenched (MILC)

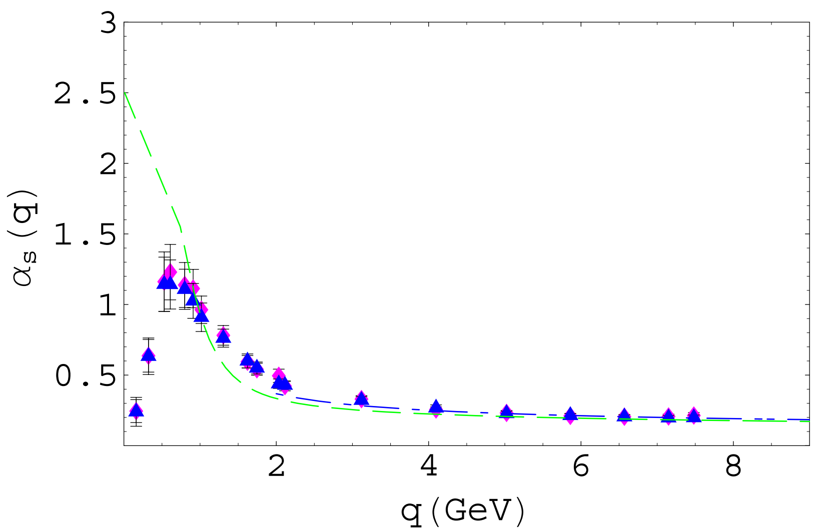

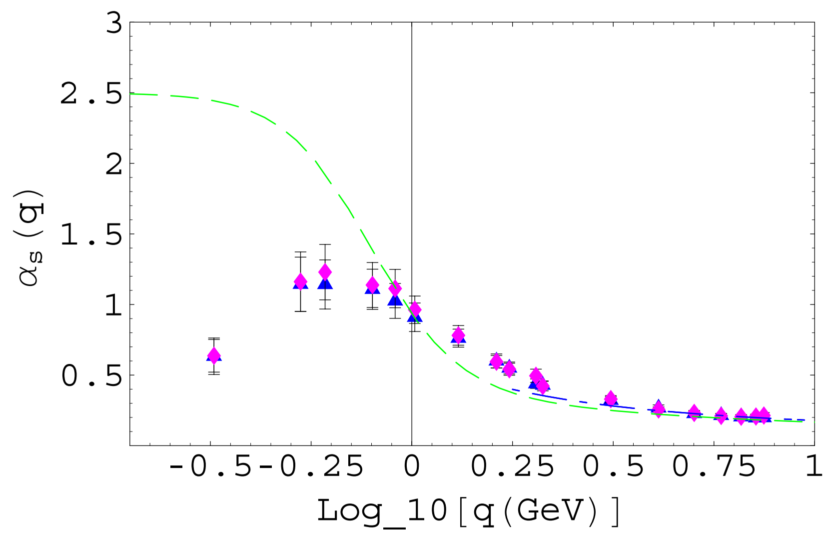

Fig.20a: $\alpha_s(q)$ of the MILC $\beta_{imp} = 6.83, am_{u,d} = 0.040$(diamonds) and $6.76, am_{u,d} = 0.007$, $am_s = 0.050$ (triangles). (50 samples)

Fig.20b: Same as Fig 20a. as the function of $\log_{10}[q(GeV)]$

- $\alpha_s(q)$, Unquenched (KS)

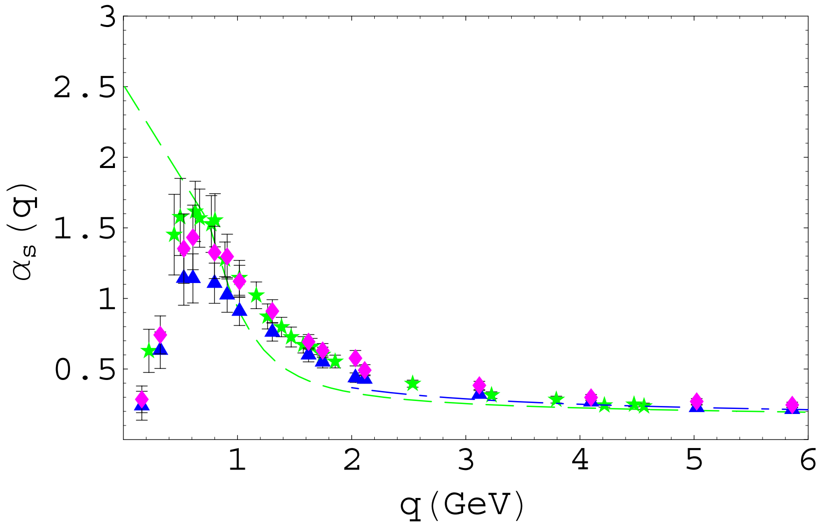

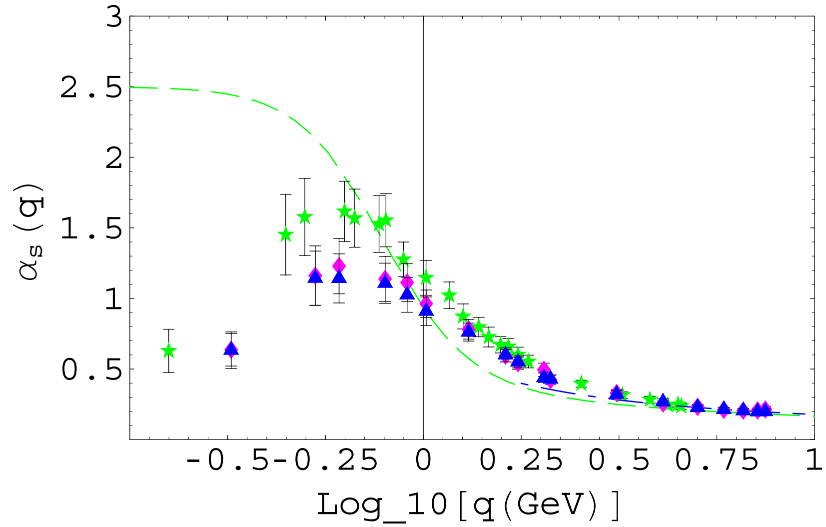

Fig.20c: $\alpha_s(q)$ of the MILC $\beta_{imp} =$ 6.83, $am_{u,d} =$ 0.040(diamonds) and 6.76, $am_{u,d} =$ 0.007, $am_s =$ 0.050 (triangles)(50 samples) and $\beta =$ 5.415, $am_{u,d} =$ 0.025 (star)(40 samples)

Fig.20d: Same as Fig 20c. as the function of $\log_{10}[q(GeV)]$

- The quark mass dependence of $\tilde{Z}_1^2$

Table 4: The $\tilde{Z}_1^2$ factor of the unquenched SU(3).

config.	heavy	light	comments
JLQCD	0.969(80)	0.986(36)	$\kappa_{sea} = 0.1340, 0.1355$
CP-PACS	1.072(76)	1.210(98)	$\kappa_{sea} = 0.1357, 0.1382$
MILC	0.826(65)	0.858(64)	$\beta_{imp} = 6.76, 6.83$
ILDG		1.226(110)	$\beta = 5.415$

IX. $\tilde{Z}_1$ of the lattice

- The renormalization point $\mu \sim 6 GeV$ for SU(3), $\mu \sim 3.0 GeV$ for SU(2).

$$\alpha_R(\mu^2) F_R(q^2,\mu^2) {J_R}^2(q^2) = \frac{\alpha_0(\Lambda_{UV})}{\tilde{Z}_1^2(\beta,\mu)} F_B(q^2,\mu^2) {J_B}^2(q^2) \quad (20)$$

$$\alpha_R(q^2) = \alpha_R(\mu^2) F_R(q^2,\mu^2) {J_R}^2(q^2) \quad (21)$$

$$F_R(q^2,\mu^2) = {Z_3}^{-1}(\beta,\mu) F_B(\beta,q^2) \quad (22)$$

$$Z_3(\beta,\mu) \propto (-\log(\sigma a^2)+\omega)^\gamma, \quad \tilde{Z}_3(\mu, m_{sea}) \sim const \quad (23)$$

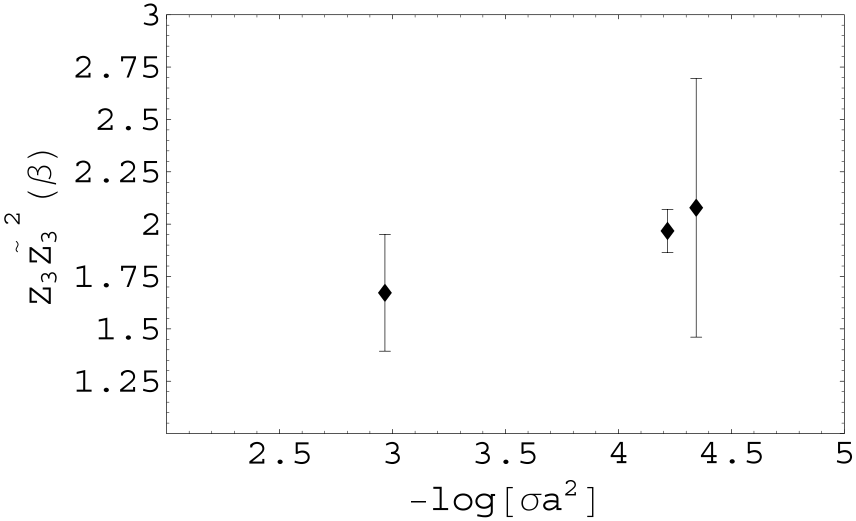

Fig.21: $Z_3\tilde{Z}_3^2$ of SU(3).

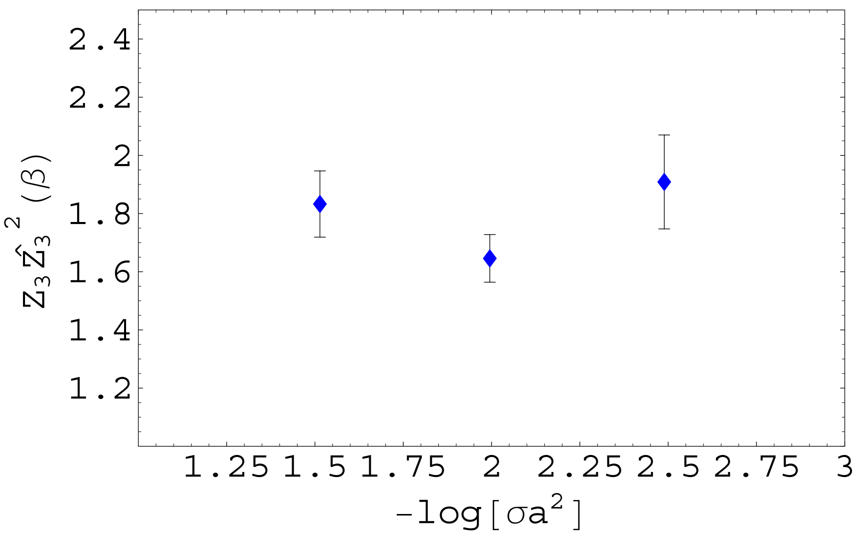

Fig.22: $Z_3\tilde{Z}_3^2$ of SU(2).

β dependence of $Z_3(\mu^2)$ is obscure.

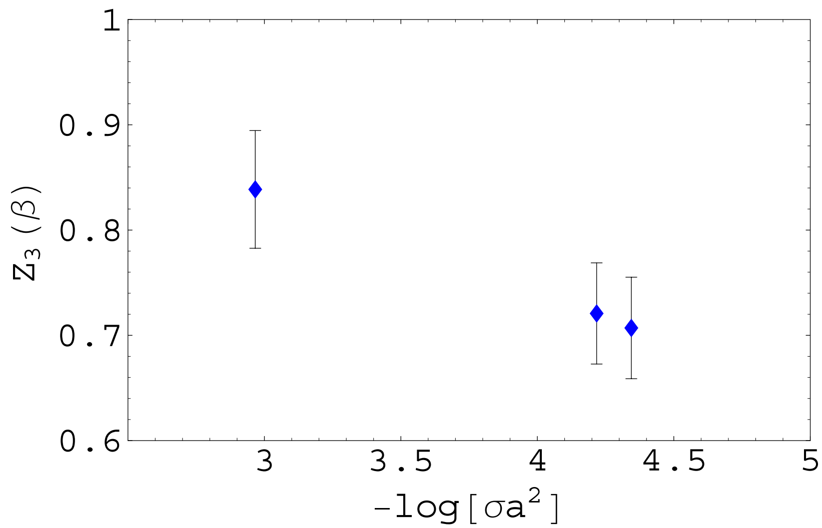

Fig.23: The gluon wave function renormalization factor $Z_3(\mu^2)$ as the function of $-\log[\sigma a^2]$. $\beta = 6.0(32^4)$, $\beta = 6.4$ and 6.45 (56^4).

X. Discussion and Conclusion

- The ghost propagator scales irrespective of quenched or unquenched(small quark mass) in the present acculacy. The string tension and the ghost propagator are correlated. Dependence of $\tilde{Z}_3(\mu^2)$ on β is weak but m_{sea} dependent.

- When $\beta \geq 6.4$, Quenched SU(3) gluon propagator obtained by the cylinder cut becomes suppressed as the lattice size L becomes large (We scaled at $\mu = 9.5 GeV$ to Orsay data.).

- The ghost propagator in $U-$linear definition is about 14% larger than that of the $\log U$ definition, but the slope α_G is the same.

- Sample wise rotational symmetry violation causes a correlation between reflection positivity violating axis and the large component of the Kugo-Ojima parameter.

- Exceptional samples ($c \sim 1$, large α_G and sample-wise manifest violation of reflection positivity), appear more frequently in the finer lattice. The suppression of the running coupling at infrared becomes mild.

- c/q^2 term in $\alpha_s(q)$ is confirmed.

- No ghost condensation in Landau gauge.

- In Unquenched SU(3), violation of Z(4) symmetry to Z(3) symmetry due to different length of the lattice axes makes the evaluation of the infrared Kugo-Ojima parameter and the running coupling uncertain.

- pQCD fits $\alpha_s(q)$ data for $q > 3GeV$. c/q^2 term is not confirmed.

- Kugo-Ojima parameter depends on whether the gauge field couples to matter or not.

- Rotational symmetry of gluon is recovered by the coupling to the matter field.

- Infrared fixed point of $\alpha_0 \sim 2.5$, $\kappa \sim 0.5$ is suggested in quenched and in unquenched chiral limit.

- Anti-screening effect is suppressed when the sea quark mass is large.

- The running coupling of 2+1 species MILC is fairly smaller than that of 2 species CP-PACS. In order to discuss different features of fermionic treatment, further detailed investigation is required.

- Similarity of the $\alpha_s(q)$ of the lattice and that of the model of dynamical chiral symmetry breaking (Higashijima) suggests a possibility of a unified description of the confinement and the chiral symmetry breaking.

- The parameter κ at $q = 0$ and α_G at around $q = 0.4GeV$ may differ by about a factor 2. Lattice data $\alpha_G \sim 0.23$ is consistent with $\kappa = 0.5$.

- There are DSE and ERGE that claim $\kappa = 0.595\cdots$, $\alpha_0 = 2.971\cdots$, and vanishing $Z_3(0)$. Existing lattice data (quenched 56^4 and unquenched after cone-cut) are incompatible with this prediction.

Phase structure in lattice QCD. (Iwasaki)

- $7 \leq N_f \leq 16$: non trivial infrared fixed point but no quark confinement.

- $N_f \leq 6$: quark confinement and spontaneous chiral symmetry breaking.

Phase structure in analytical perturbation theory.(Grunberg)

- $N_f \geq 10$: perturbative phase.

- $0 \leq N_f \leq 10$: $\alpha_0 \sim \dfrac{4}{11 - (2/3)N_f}$

References

[1] V.N. Gribov, Nucl. Phys. **B 139**1(1978).

[2] T. Kugo and I. Ojima, Prog. Theor. Phys. Suppl. **66**, 1 (1979).

[3] D. Zwanziger, Nucl. Phys. **B 364** ,127 (1991), idem B **412**, 657 (1994).

[4] D. Zwanziger, Phys. Rev. D**69**,016002(2004), arXiv:hep-ph/0303028.

[5] A. Cucchieri, Nucl. Phys. **B521**,365(1998), arXiv:hep-lat/9711024.

[6] S. Furui and H.Nakajima, Phys. Rev. D**69**,074505(2004) and references therein, hep-lat/0305010.

[7] S. Furui and H.Nakajima, Phys. Rev. D**70**,094504(2004) and references therein, hep-lat/0403021.

[8] S.Aoki et al., (JLQCD collaboration), Phys. Rev. D**65**,094507(2002); ibid Phys. Rev. D**68**,054502(2003).

[9] A. Ali Khan et al., (CP-PACS collaboration), Phys. Rev. D**65**,054505(2002); S.Aoki et al.,(CP-PACS collaboration), PRD**60**,114508(

[10] C.W. Bernard et al., (MILC collaboration), Phys. Rev. D**64**,054506(2001).